PAPER

Check for updates

Synthesis and self-assembly of a penta[60]fullerene bearing benzo[*ghi*]perylenetriimide units†

Clément Drou,[a] Théo Merland,[b] Antoine Busseau,[a] Sylvie Dabos-Seignon, [ID] [a] Antoine Goujon, [ID] [a] Piétrick Hudhomme, [ID] [a] Lazhar Benyahia, [ID] [b] Christophe Chassenieux [ID] *[b] and Stéphanie Legoupy [ID] *[a]

A benzo[*ghi*]perylenetriimide (BPTI) derivative bearing a terminal azido group on the expanded π-conjugated backbone has been synthesized and characterized. This promising photo- and electroactive BPTI motif has been used to obtain an original penta(organo)fullerene as a promising multi-electron acceptor system. Our studies show its self-assembly resulting from aggregation *via* π–π stacking interaction in solution and in the solid state.

Introduction

Perylenediimide (PDI) derivatives are well-known organic dyes with outstanding thermal, chemical and photostability properties.[1] Thanks to their strong electron-accepting ability, ease of functionalization,[2,3] and high electron mobility,[4,5] PDIs are promising n-type organic semiconductors which have been widely used in organic electronic and optoelectronic devices.[6–9] They have also gained interest as building blocks for supramolecular polymers.[10]

A new class of acceptor molecules has recently emerged with benzo[*ghi*]perylenetriimide (BPTI) derivatives. In comparison with the structure of PDI, their π-conjugated system is laterally expanded by a five-membered imide ring. BPTI chromophore shows a blue-shifted absorption and a stronger solid state fluorescence[11] compared to that of PDI. This π-extended BPTI backbone has very recently been studied in perovskite solar cells as electron transporting layer,[12] organic–lithium redox-flow batteries,[13] photocatalytic degradation of pollutants,[14] single component organic solar cells (SCOSC)[15] and devices for artificial photosynthesis in water splitting.[16] Moreover a BPTI derivative has been used in supramolecular chemistry affording a 1 : 1 supramolecular complex with zinc porphyrin through hydrogen bonds and an ultrafast photo-induced electron transfer occurred between the two columns of donors and BPTI acceptors.[17]
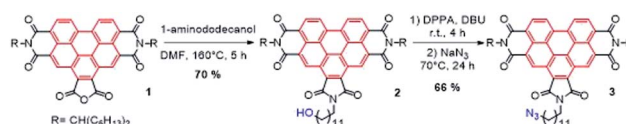
Fullerene C$_{60}$ thanks to its tridimensional structure and excellent electron accepting properties[18] has been widely used in the formation of supramolecular polymeric nano-network. In particular, the pentasubstituted fullerenes developed by Nakamura and co-workers are well suited. The conical structure obtained by regioselective pentafunctionalization of C$_{60}$ offers remarkable self-assembly capabilities.[19–24] Recently, we reported the syntheses of penta(organo)[60]fullerenes using five tetrathiafulvalene[25] (TTF) or (Zn)porphyrin[26] fragments as electroactive recognition units which led, thanks to π–π and electronic interactions, to supramolecular arrangements similar to shuttlecocks nested into each other. With the aim of developing new supramolecular assembly based on penta(organo)[60]fullerenes, we were interested in the use of the self-aggregative BPTI motifs to assemble fullerene derivatives.

Results and discussion

We first synthesized a BPTI derivative bearing an azido terminal group to be clicked to a penta(organo)[60]fullerene by using the highly efficient so-called CuAAC (copper-catalysed azide–alkyne cycloaddition) reaction.[27]

BPTI azide **3** was synthesized in two steps starting from benzo[*ghi*]perylenediimide (BPDI) **1** prepared according to reported procedure.[28] The imidization reaction was carried out using 1-aminododecanol on the anhydride function of BPDI **1** affording BPTI **2**. Then, a nucleophilic substitution on the hydroxyl group using sodium azide after activation with diphenylphosphoryl azide[29] led to BPTI azide **3** (Scheme 1).

[a]Laboratoire MOLTECH-Anjou, UMR CNRS 6200, Univ. Angers, SFR Matrix, 2 Bd Lavoisier, 49045 Angers Cedex, France. E-mail: Stephanie.Legoupy@univ-angers.fr
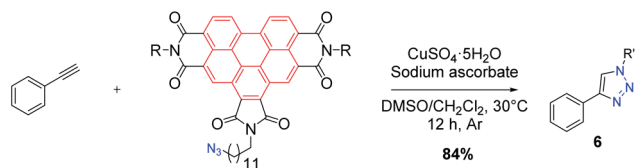
[b]Institut des Molécules et Matériaux du Mans, UMR CNRS 6283, Le Mans Univ., 1, Av Olivier Messiaen, 72085 Le Mans Cedex 9, France. E-mail: christophe.chassenieux@univ-lemans.fr

† Electronic supplementary information (ESI) available. See DOI: 10.1039/d1ra00287b

Scheme 1 Synthesis of BPTI-azide **3**.
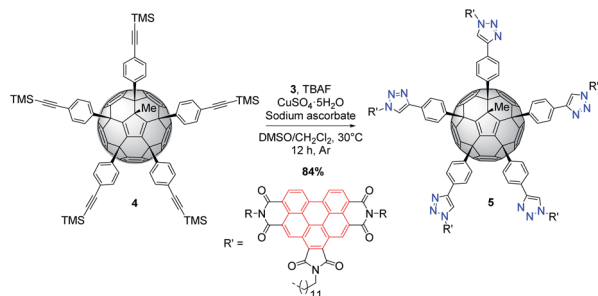
Scheme 2   Synthesis of penta(BPTI)[60]fullerene **5**.

Scheme 3   Synthesis of the reference molecule **6**.

BPTI **3** was then clicked to penta(TMS)[60]fullerene[30] **4** under CuAAC conditions. Compound **4** was first desilylated *in situ* with tetrabutylammonium fluoride (TBAF)[31] to provide the corresponding terminal alkyne and reaction with excess of azide **3** afforded desired penta(BPTI)[60]fullerene **5** in a remarkable 84% yield, resulting from five one-pot cycloadditions. The latter can be assimilated to a central fullerene surrounded by five BPTI "arms" (shuttlecock type) (Scheme 2).

Reference molecule **6** was also synthesized using CuAAC click reaction between BPTI azide **3** and phenylacetylene (Scheme 3).

The structure of compounds **5** and **6** were confirmed by their ^{1}H, ^{1}H–^{1}H COSY and ^{13}C NMR spectra (Fig. S1–S10†) as well as by HR MALDI-TOF mass spectrometry (Fig. S16–S19†). The purity of penta(BPTI)[60]fullerene could be estimated to be higher than 99.5% thanks to HPLC analysis (Fig. S20†).
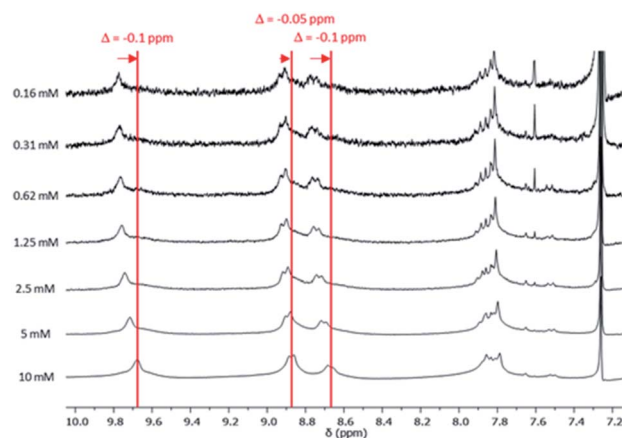

Fig. 1 ^{1}H NMR spectra of compound **5** at different concentrations (0.16–10 mM) between 7.1 and 10.1 ppm (phenyl aromatic region) in CDCl$_3$ at 25 °C.
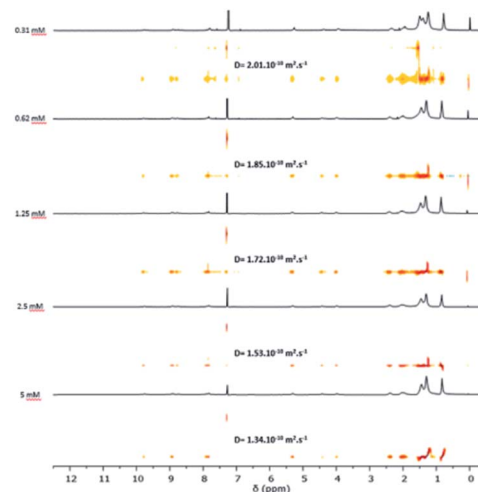

Fig. 2 ^{1}H DOSY NMR spectrum (300 MHz, CDCl$_3$, 298 K) of penta(BPTI)[60]fullerene **5** at different concentrations.

The self-assembly of these derivatives has been investigated, both in solution and solid state, by NMR spectroscopy, electrochemical analyses, mass spectrometry, atomic force microscopy (AFM) and combined dynamic/static light scattering (DLS/SLS).

^{1}H NMR spectra of compound **5** was recorded at different concentrations between 0.16 and 10 mM (CDCl$_3$, 25 °C; Fig. 1 and S11†). A downfield shift of the aromatic protons is observed when the concentration increases (−0.1 ppm), suggesting the aggregation of BPTI units. On the contrary, no change could be observed in the chemical shift of the triazole protons. As expected by the introduction of the dodecyl spacer length, the triazole ring seems not to be involved in such an aggregation phenomenon (Fig. 1).

Complementary ^{1}H DOSY NMR experiments on compound **5** were performed between 0.31 and 5 mM in CDCl$_3$ (Fig. 2). A decrease of the self-diffusion coefficient D_s was observed when the concentration increases which is in agreement with the formation of aggregates.

Using the Stokes–Einstein equation (eqn (S8)†), the hydrodynamic radius of the objects was estimated to be between 2 and 3 nm depending on the concentration (Table 1).

Similar analysis was carried out with reference molecule **6** (Fig. 3 and S13†). ^{1}H NMR spectra at different concentrations

Table 1   Self-diffusion coefficients (D_s) and hydrodynamic radii (r) of aggregates of **5** at different concentrations estimated from the Stokes–Einstein equation (eqn (S8)) using ^{1}H DOSY NMR data

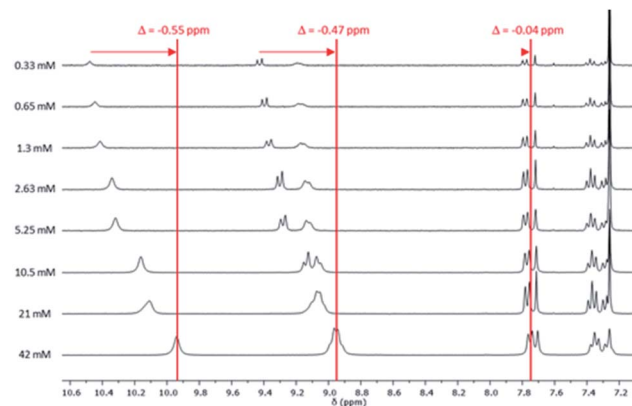| [C] (mM)	D_s (m^2 s^{-1})	r (Å)
0.31	2.01×10^{-10}	20
0.62	1.85×10^{-10}	22
1.25	1.72×10^{-10}	23
2.5	1.53×10^{-10}	26
5	1.34×10^{-10}	30

Fig. 3 ¹H NMR spectra of reference **6** at different concentrations (0.33–42 mM) between 7.1 and 10.5 ppm (phenyl aromatic region) in CDCl₃ at 25 °C.

(between 0.33 mM and 42 mM) showed a downfield shift of the aromatic protons five times higher than the one obtained for pentaadduct **5**. This suggests that π–π stacking governs the weak interaction involved in the self-assembly of reference **6**. A downfield shift of the third imide proton (−0.02 ppm) was also noticed while an upfield shift of the protons of the symmetrical diimide (+0.04 ppm) was observed (Fig. S12†).

These results allowed us to propose a hypothesis concerning the interactions arising in the assembly of pentaadduct **5**. Indeed, we can assume that the BPTI cores are aggregating via π–π stacking and that the fullerene unit is not involved in such assembly. Additional NMR experiments were performed to confirm this assumption. Indeed, the mixture of compound **6** with fullerene C₆₀ or with compound **4** did not display a significant shift of the aromatic protons even at increased concentrations (Fig. S14 and S15†).

Aggregation of penta(BPTI)[60]fullerene **5** in solution was confirmed by both static and dynamic light scattering measurements. Fig. 4a displays the concentration dependence of the cooperative diffusion coefficient (Dᶜ) for compound **5** measured by DLS which probed a single diffusive mode of relaxation (Fig. S25†). The Dᶜ value is in close agreement with
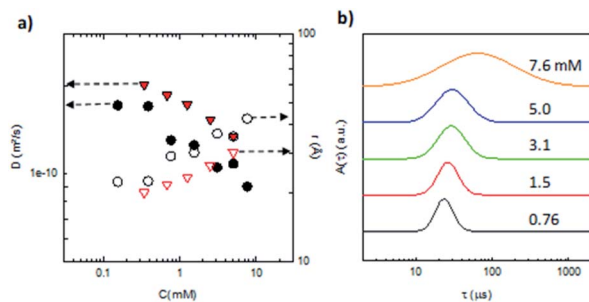

Fig. 4 (a) Diffusion coefficients (filled symbols) and hydrodynamic radii (empty symbols) of compound **5** calculated from DLS (●) and DOSY NMR (▼) measurements. (b) Distribution of relaxation times measured at 90° for various concentrations of compound **5** in chloroform as labelled on the figure.

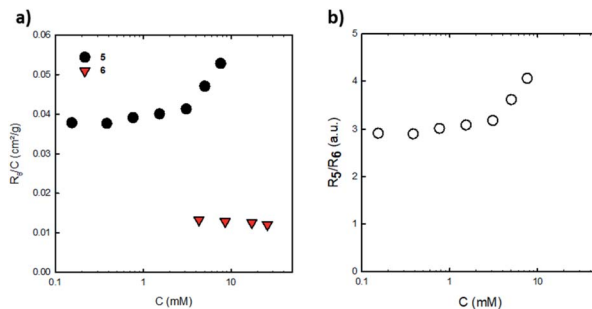**Fig. 5** (a) Rayleigh ratios normalized by concentration for solutions of penta(BPTI)[60]fullerene **5** and reference **6** in CHCl₃ at 20 °C. (b) Ratio of Rayleigh ratios of **5** and **6** against **5** concentration.

the one of Dₛ obtained from DOSY NMR measurements from both the point of view of its magnitude and concentration dependence. Upon increasing the concentration of penta(BPTI)[60]fullerene **5**, there is a clear shift of the distribution of sizes derived from DLS (Fig. 4b and S24†) towards higher values (from 2 up to 4 nm) and also a broadening of these distributions, both facts accounting for aggregation of compound **5** in solution. However we noticed that this association led to aggregates of small size over the whole concentration range investigated.

An estimation of the aggregation number of compound **5** thanks to SLS measurements may be attempted. First, it should be mentioned that solutions of C₆₀ and compound **4** did not scatter light in chloroform which meant that their contrast is very small and that only BPTI units contribute to the scattered intensity for solutions of compounds **5** and **6** in the same solvent. Solutions of penta(BPTI)[60]fullerene **5** scatter much more than solutions of reference **6** at the same concentration (Fig. 5).

The ratio in their scattering intensities is then related to the number of BPTI units involved which should be five if both compounds **5** and **6** were not aggregated in chloroform. The ratio of scattered intensity between compounds **5** and **6** ranges from three up to four meaning that 5 in chloroform is at least three times more aggregated than reference **6**. However, the aggregation number of **6** in chloroform is unknown but as evidenced from NMR, **6** is far from being at the unimer state in the concentration range investigated. It can then be concluded that the penta(BPTI)[60]fullerene **5** is aggregated in chloroform and that its aggregation number is at least three times higher than the reference BPTI **6** at the same concentration.

AFM studies were carried out to investigate the self-assembly of penta(BPTI)[60]fullerene **5** in solid state. Solutions with concentration ranging from 0.2 to 0.6 mM were spin coated onto glass substrate. The AFM images showed aggregates which height is mainly 3–4 nm (Fig. 6, S28 and S29†), with some up to 9 nm, in line with the self-assembly of several molecules as evidenced from other techniques.

In the case of reference molecule **6** no obvious assembly was observed, as shown in Fig. S30.† AFM succeeded in proving the self-assembly of penta(BPTI)[60]fullerene **5** in solid state but results for reference **6** were less conclusive.
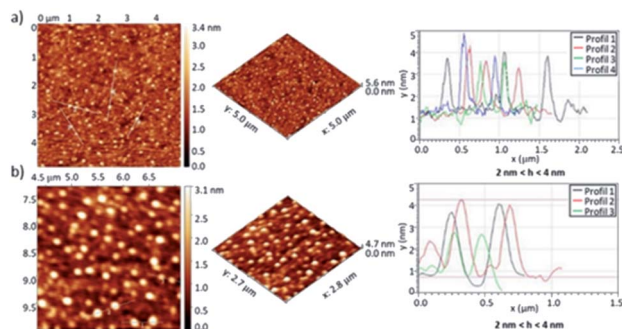
© 2021 The Author(s). Published by the Royal Society of Chemistry

Fig. 6 AFM images of penta(BPTI)[60]fullerene 5 in 2D and 3D at 0.4 mM, spin coated onto glass substrate and associated profiles. (a) 5 μm × 5 μm scan (b) magnification of (a).
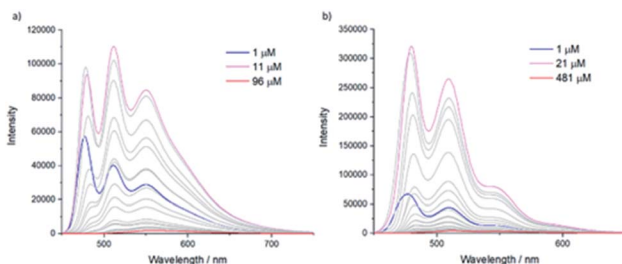

Fig. 7 Concentration-dependent fluorescence spectra of (a) penta(BPTI)[60]fullerene 5 (addition of 5 μM per spectrum), region 450–750 nm and (b) reference 6 (addition of 10 μM per spectrum until 201 μM and then 20 μM per spectrum), region 450–650 nm, CHCl$_3$, λ_{exc} = 467 nm, 298 K, 1 cm cuvette. Pink curves: concentration corresponding to the maximum of emission intensity.

Fig. 8 Concentration-dependent fluorescence spectra of compounds 4 + 6 (in a molar ratio 1 : 5 of 4 and 6, respectively), region 400–800 nm, CHCl$_3$, λ_{exc} = 467 nm, 298 K, 1 cm cuvette, addition of 10 μM of compound 4 and 50 μM of reference 6 per spectrum. Pink curve: concentration corresponding to the maximum of emission intensity. The legend displays concentration of 4.

The emission spectra of 5 in chloroform were measured at different concentrations (Fig. 7a). From 1 μM to 11 μM the emission intensity increased with the concentration. Interestingly, an extinction of the luminescence of penta(BPTI)[60] fullerene 5 was then observed until 96 μM. Since the fullerene is not involved in the assembly, this quenching can be related to the aggregation of the molecule *via* BPTI–BPTI interaction.

Identical measurements were performed on reference molecule 6 (Fig. 7b). The same behaviour was observed except that the concentration at which the extinction appears was much higher. Indeed, if we compare in terms of BPTI units (*i.e.* BPTI concentration in solution), the extinction concentration in penta(BPTI)[60]fullerene 5 was 2.2 μM against 21 μM for reference 6. Thus, the luminescence quenching is facilitated in compound 5.

In order to confirm the difference between compounds 5 and 6, additional analyses were performed by mixing reference 6 with compound 4 according to a ratio 5/1 which simulated 5 (Fig. 8). The resulting spectrum was comparable to this from reference 6 alone, suggesting that fullerene does not govern the formation of the assembly. On the contrary, the conformation of the BPTI arms in 5 favours the aggregation. Indeed, the pentafullerene scaffold, with the five arms sufficiently close to each other, seems to enhance the BPTI–BPTI interactions.

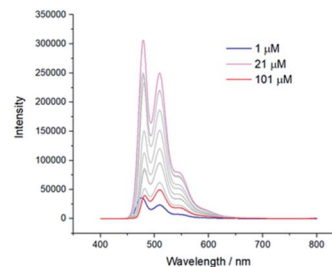The absorption properties of both compounds 5 and 6 were also studied (Fig. S21–S23†). Concerning reference 6, the band in the 400–500 nm region is typically assigned to the S$_0$ → S$_1$ optical transition of BPTI and the band in the 350–400 nm region is attributed to the S$_0$ → S$_2$.[11,15] The absorption spectrum of penta(BPTI)[60]fullerene 5 showed absorption bands corresponding to the addition of both fullerene and BPTI moieties, but the self-assembly phenomenon could not be observed by UV-Vis spectroscopy.

The electronic properties were investigated using cyclic voltammetry technique. Cyclic voltammograms of compounds 5 and 6 were recorded at room temperature in *o*-dichlorobenzene (*o*-DCB)/MeCN containing 0.1 M *n*Bu$_4$NPF$_6$. The voltammogram of penta(BPTI)[60]fullerene 5 consists in an average between the electronic contribution of fullerene C$_{60}$ and reference 6 (Fig. S26 and Table S1†). Successive redox couples, corresponding to the multiple reduction process of the respective BPTI unit and C$_{60}$ fragment, were observed. As shown in Fig. S27 and Table S2,† an increase of the concentration of 5 produced no shift in reduction waves. Then no electronic communication between C$_{60}$ and BPTI could be observed. Thus, C$_{60}$ can be self-assembled while preserving its electronic properties.

Conclusions

We have described in this work the synthesis of a benzo[*ghi*] perylenetriimide (BPTI) derivative bearing an azido group which was clicked using the CuAAC reaction to a penta(organo) fullerene. Using different techniques, we have shown the existence of π–π stacking interactions between the BPTI arms leading to aggregation of the pentaadduct. This aggregation is concentration dependent as evidenced from LS, AFM, fluorescence and NMR measurements. Moreover, this original penta(BPTI)[60]fullerene presents multi-redox accepting properties opening the way to innovative applications in materials science.

Experimental section

General procedure for the synthesis of compound 2

A solution of BPDI 1 (800 mg, 0.94 mmol) and 1-amino-dodecanol (380 mg, 1.88 mmol) in DMF (20 mL) was refluxed for 5 hours. The solvent was evaporated under vacuum and the crude was purified by chromatography (silica gel, CHCl$_3$

followed by 2% v/v MeOH in CHCl$_3$). A second chromatography column (neutral aluminium oxide, CHCl$_3$ followed by 2% v/v MeOH in CHCl$_3$) was necessary for completing purification and gives the desired product as an orange solid (700 mg, 72% yield). ^{1}H NMR (300 MHz, CDCl$_3$) δ ppm: 10.30 (s, 2H), 9.26 (d, J = 8.3 Hz, 2H), 9.11 (d, J = 8.0 Hz, 2H), 5.31 (s, 2H), 3.98 (t, J = 5.9 Hz, 2H), 3.63 (t, J = 6.60 Hz, 2H), 2.50–2.26 (m, 4H), 2.06–1.82 (m, 6H), 1.71–1.18 (m, 51H), 0.92–0.77 (m, 12H). ^{13}C NMR (125 MHz, CDCl$_3$) δ ppm: 168.1, 132.8, 129.9, 127.4, 127.3, 127.1, 125.4, 124.4, 123.7, 122.9, 120.2, 63.2, 55.5, 38.8, 33.0, 32.6, 32.0, 29.5, 28.8, 17.3, 27.1, 25.9, 22.8, 14.2. HRMS (MALDI-TOF, negative mode): calcd for C$_{66}$H$_{85}$N$_3$O$_7$ 1031.6388 [M]$^-$; found 1031.6385.

General procedure for the synthesis of compound 3

A solution of compound **2** (300 mg, 0.29 mmol) in dry DMF (30 mL) was stirred under argon bubbling for 5 minutes. DPPA (0.62 mL, 1.45 mmol) and DBU (45 μL, 0.29 mmol) were added and the solution was stirred at room temperature for 5 hours under argon atmosphere. NaN$_3$ (96 mg, 1.45 mmol) was added and the mixture was stirred at 70 °C for 24 hours. The product was extracted with CHCl$_3$ (200 mL), then the organic layer was washed with brine (3 × 200 mL), dried over MgSO$_4$ and concentrated under reduced pressure. The crude mixture was purified by two successive chromatography columns using respectively silica gel (CHCl$_3$) and neutral aluminium oxide (CHCl$_3$ followed by 2% v/v MeOH in CHCl$_3$) affording the desired product as an orange solid (204 mg, 66% yield). ^{1}H NMR (300 MHz, CDCl$_3$) δ ppm: 10.36 (s, 2H), 9.31 (d, J = 8.58 Hz, 2H), 9.14 (d, J = 7.70 Hz, 2H), 5.32 (s, 2H), 3.98 (t, J = 7.25 Hz, 2H), 3.24 (t, J = 6.95 Hz, 2H), 2.48–2.26 (m, 4H), 2.12–1.8 (m, 6H), 1.67–1.14 (m, 50H), 0.94–0.75 (m, 12H). ^{13}C NMR (125 MHz, CDCl$_3$) δ ppm: 168.4, 133.3, 130.8, 130.4, 130.1, 129.6, 127.7, 124.9, 124.0, 123.4, 55.4, 51.6, 38.8, 32.6, 32.0, 31.6, 30.4, 29.9, 29.8, 29.7, 29.6, 29.4, 29.3, 29.0, 28.9, 27.2, 27.1, 26.9, 22.8, 14.2. HRMS (MALDI-TOF, negative mode): calcd for C$_{66}$H$_{84}$N$_6$O$_6$ 1056.6452 [M]$^-$; found 1056.6467.

General procedure for the synthesis of compound 5

Tetrabutylammonium fluoride (TBAF; 1 M in THF, 0.12 mL, 0.14 mmol) was added to a solution of penta(TMS)-2-methyl[60] fullerene **4** (ref. 32) (8 mg, 5 μmol), freshly prepared azido compound **3** (42 mg, 40 μmol), CuSO$_4$·5H$_2$O (0.25 mg, 0.9 μmol), and sodium ascorbate (3.6 mg, 18 μmol) in 3 mL of DMSO/CH$_2$Cl$_2$ (1 : 2, v/v). The mixture was stirred at room temperature for 24 hours. Then the solution was diluted with CHCl$_3$ (100 mL), washed with a saturated NH$_4$Cl aqueous solution (1 × 100 mL) and water (2 × 100 mL), dried with MgSO$_4$, filtered, and concentrated under vacuum. The crude product was purified by chromatography (silica gel, CHCl$_3$ followed by 2% v/v MeOH in CHCl$_3$) and centrifuged in CHCl$_3$/MeCN to afford penta(BPTI)[60]fullerene **5** as a bright orange solid (27 mg, 84% yield). ^{1}H NMR (300 MHz, CDCl$_3$) δ ppm: 9.71 (s, 10H), 8.89 (m, 10H), 8.71 (m, 10H), 7.86–7.79 (m, 20H), 7.69–7.46 (m, 5H), 5.31 (s, 10H), 4.54–4.25 (m, 10H), 3.99 (m, 10H), 3.64 (s, 1H), 2.50–2.32 (m, 20H), 2.15–1.82 (m, 40H), 1.62–1.20

(m, 242H), 0.93–0.80 (m, 60H). ^{13}C NMR (125 MHz, CDCl$_3$) δ ppm: 167.6, 164.3, 163.6, 163.3, 162.4, 161.8, 160.5, 159.7, 157.0, 152.9, 151.8, 148.8, 148.7, 148.6, 148.5, 148.4, 148.3, 147.9, 147.8, 147.4, 147.2, 146.9, 145.7, 145.5, 144.9, 144.5, 144.4, 144.2, 144.0, 143.8, 142.9, 142.7, 139.4, 139.0, 137.8, 132.0, 130.7, 130.6, 130.5, 129.3, 128.8, 127.0, 126.7, 126.4, 126.2, 126.1, 126.0, 125.6, 125.3, 124.8, 123.6, 123.5, 123.1, 122.8, 122.1, 120.2, 120.1, 119.7, 62.6, 62.5, 61.0, 58.2, 55.5, 50.7, 50.6, 38.9, 33.6, 32.6, 32.0, 30.6, 29.8, 29.7, 29.5, 29.4, 29.2, 28.8, 27.3, 26.8, 26.7, 24.9, 22.8, 14.3. HRMS (MALDI-TOF, negative mode): calcd for C$_{431}$H$_{448}$N$_{30}$O$_{30}$ 6523.4453 [M]$^-$; found 6523.4926. HPLC analysis: retention time = 3.96 min (eluent: toluene, flow rate: 1 mL min^{-1}, wavelength: 320 nm).

General procedure for the synthesis of compound 6

CuSO$_4$·5H$_2$O (1 mg, 4 μmol) and sodium ascorbate (10 mg, 50 μmol) were added to a solution of (phenylethynyl)trimethylsilane (24 μL, 0.22 mmol) and freshly prepared compound **3** (117 mg, 0.11 mmol) in a mixture of DMSO (2 mL) and CH$_2$Cl$_2$ (4 mL). The solution was stirred at room temperature overnight. The mixture was subsequently diluted with CH$_2$Cl$_2$ and washed with a saturated NH$_4$Cl aqueous solution (1 × 100 mL), brine (1 × 100 mL) and water (1 × 100 mL). The organic phase was dried (MgSO$_4$), filtered and concentrated under vacuum. The crude was purified by gel chromatography (silica gel, 2% v/v MeOH in CHCl$_3$) to obtain the desired compound as an orange solid (108 mg, 84% yield). ^{1}H NMR (300 MHz, CDCl$_3$) δ ppm: 9.95 (s, 2H), 8.97 (s, 4H), 7.76 (d, J = 7.35 Hz, 2H), 7.71 (s, 1H), 7.35 (t, J = 7.20 Hz, 2H), 7.3–7.26 (m, 1H), 5.32 (s, 2H), 4.38 (t, J = 7.28 Hz, 2H), 4.00 (t, J = 7.37, Hz, 2H), 2.48–2.30 (m, 4H), 2.11–1.99 (m, 4H), 1.98–1.83 (m, 4H), 1.60–1.20 (m, 48H), 0.88–0.82 (m, 12H). ^{13}C NMR (125 MHz, CDCl$_3$) δ ppm: 167.9, 147.8, 132.5, 130.8, 128.9, 128.1, 127.2, 127.1, 126.8, 125.7, 124.1, 132.6, 122.7, 119.4. HRMS (MALDI-TOF, negative mode): calcd for C$_{74}$H$_{90}$N$_6$O$_6$ 1158.6922 [M]$^-$; found 1158.6923.

Conflicts of interest

There are no conflicts to declare.

Acknowledgements

Notes and references

1 H. Langhals, *Heterocycles*, 1995, **40**, 477–500.
2 C. Huang, S. Barlow and S. R. Marder, *J. Org. Chem.*, 2011, **76**, 2386–2407.

3 A. Nowak-Król and F. Würthner, *Org. Chem. Front.*, 2019, **6**, 1272–1318.

4 Y. Liu, Y. Wang, L. Ai, Z. Liu, X. Ouyang and Z. Ge, *Dyes Pigm.*, 2015, **121**, 363–371.

5 S. Naqvi, M. Kumar and R. Kumar, *ACS Omega*, 2019, **4**, 19735–19745.

6 Z. Guo, X. Zhang, Y. Wang and Z. Li, *Langmuir*, 2019, **35**, 342–358.

7 S. Chen, P. Slattum, C. Wang and L. Zang, *Chem. Rev.*, 2015, **115**, 11967–11998.

8 A. L. Briseno, S. C. B. Mannsfeld, C. Reese, J. M. Hancock, Y. Xiong, S. A. Jenekhe, Z. Bao and Y. Xia, *Nano Lett.*, 2007, **7**, 2847–2853.

9 W. Huang, J. C. Markwart, A. L. Briseno and R. C. Hayward, *ACS Nano*, 2016, **10**, 8610–8619.

10 C. Jarrett-Wilkins, X. He, H. E. Symons, R. L. Harniman, C. F. J. Faul and I. Manners, *Chem.–Eur. J.*, 2018, **24**, 15556–15565.

11 H. Langhals and S. Kirner, *Eur. J. Org. Chem.*, 2000, 365–380.

12 P. Karuppuswamy, H.-C. Chen, P.-C. Wang, C.-P. Hsu, K.-T. Wong and C.-W. Chu, *ChemSusChem*, 2018, **11**, 415–423.

13 L. Li, H.-X. Gong, D.-Y. Chen and M.-J. Lin, *Chem.–Eur. J.*, 2018, **24**, 13188–13196.

14 S. Zhang, H. Guo, W. Hou, X. Ji and H. Zhang, *Mater. Lett.*, 2018, **221**, 38–41.

15 F. Yang, J. Li, C. Li and W. Li, *Macromolecules*, 2019, **52**, 3689–3696.

16 H.-C. Chen, C.-P. Hsu, J. N. H. Reek, R. M. Williams and A. M. Brouwer, *ChemSusChem*, 2015, **8**, 3639–3650.

17 H. Sakai, K. Ohkubo, S. Fukuzumi and T. Hasobe, *Chem.–Asian J.*, 2016, **11**, 613–624.

18 Q. Xie, E. Perez-Cordero and L. Echegoyen, *J. Am. Chem. Soc.*, 1992, **114**, 3978–3980.

19 Y. Matsuo, T. Ichiki and E. Nakamura, *J. Am. Chem. Soc.*, 2011, **133**, 9932–9937.

20 Y. Matsuo, K. Morita and E. Nakamura, *Chem.–Asian J.*, 2008, **3**, 1350–1357.

21 Y.-W. Zhong, Y. Matsuo and E. Nakamura, *J. Am. Chem. Soc.*, 2007, **129**, 3052–3053.

22 C. J. Tassone, A. L. Ayzner, R. D. Kennedy, M. Halim, M. So, Y. Rubin, S. H. Tolbert and B. J. Schwartz, *J. Phys. Chem. C*, 2011, **115**, 22563–22571.

23 T. Niinomi, Y. Matsuo, M. Hashiguchi, Y. Sato and E. Nakamura, *J. Mater. Chem.*, 2009, **19**, 5804–5811.

24 Y. Matsuo, A. Muramatsu, Y. Kamikawa, T. Kato and E. Nakamura, *J. Am. Chem. Soc.*, 2006, **128**, 9586–9587.

25 A. Busseau, C. Villegas, S. Dabos-Seignon, C. Cabanetos, P. Hudhomme and S. Legoupy, *Chem.–Eur. J.*, 2016, **22**, 8452–8456.

26 A. Busseau, C. Villegas, S. Dabos-Seignon, P. Hudhomme and S. Legoupy, *Eur. J. Org. Chem.*, 2018, 4860–4866.

27 E. Haldón, M. C. Nicasio and P. J. Pérez, *Org. Biomol. Chem.*, 2015, **13**, 9528–9550.

28 L. C. K. Viswanath, J. Bernhardt, K. Kumar Gnanasekaran, C. Want, J. Frank, J. Faulkner and S. Krishnan, *Dyes Pigm.*, 2016, **134**, 453–458.

29 A. S. Thompson, G. R. Humphrey, A. M. DeMarco, D. J. Mathre and E. J. J. Grabowski, *J. Org. Chem.*, 1993, **58**, 5886–5888.

30 Y.-W. Zhong, Y. Matsuo and E. Nakamura, *Org. Lett.*, 2006, **8**, 1463–1466.

31 J. Iehl and J.-F. Nierengarten, *Chem.–Eur. J.*, 2009, **15**, 7306–7309.

32 Y. W. Zhong, Y. Matsuo and E. Nakamura, *Org. Lett.*, 2006, **8**, 1463–1466.